



Engineering, Operations & Technology  
Boeing Research & Technology

Research & Technology

# Improvements in Modeling Thruster Plume Erosion Damage to Spacecraft Surfaces



Carlos Soares <sup>1</sup>  
Randy Olsen <sup>1</sup>  
Courtney Steagall <sup>1</sup>  
Alvin Huang <sup>1</sup>  
Ron Mikatarian <sup>1</sup>  
Brandon Myers <sup>1</sup>  
Steven Koontz <sup>2</sup>  
Erica Worthy <sup>2</sup>

<sup>1</sup> Boeing Research & Technology  
<sup>2</sup> NASA Johnson Space Center

13th International Symposium on Materials in the Space Environment  
June 22-26, 2015

# Introduction

Engineering, Operations & Technology | Boeing Research & Technology

- Spacecraft bipropellant thrusters impact spacecraft surfaces with high speed droplets of unburned and partially burned propellant.
  - These impacts can produce erosion damage to optically sensitive hardware and systems (e.g., windows, camera lenses, solar cells and protective coatings)
- On the International Space Station (ISS), operational constraints are levied on the position and orientation of the solar arrays to mitigate erosion effects during thruster operations
- In 2007, the ISS Program requested evaluation of erosion constraint relief to alleviate operational impacts due to an impaired Solar Alpha Rotary Joint (SARJ)
- Boeing Space Environments initiated an activity to identify and remove sources of conservatism in the plume induced erosion model to support an expanded range of acceptable solar array positions
- The original plume erosion model over-predicted plume erosion and was adjusted to better correlate with flight experiment results
- This paper discusses findings from flight experiments and the methodology employed in modifying the original plume erosion model for better correlation of predictions with flight experiment data
- The updated model has been successfully employed in reducing conservatism and allowing for enhanced flexibility in ISS solar array operations

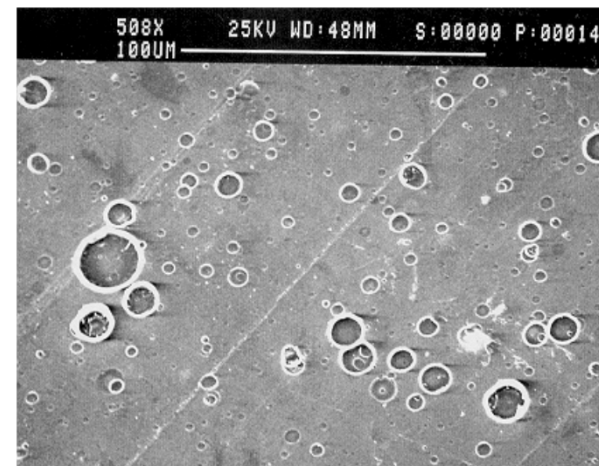
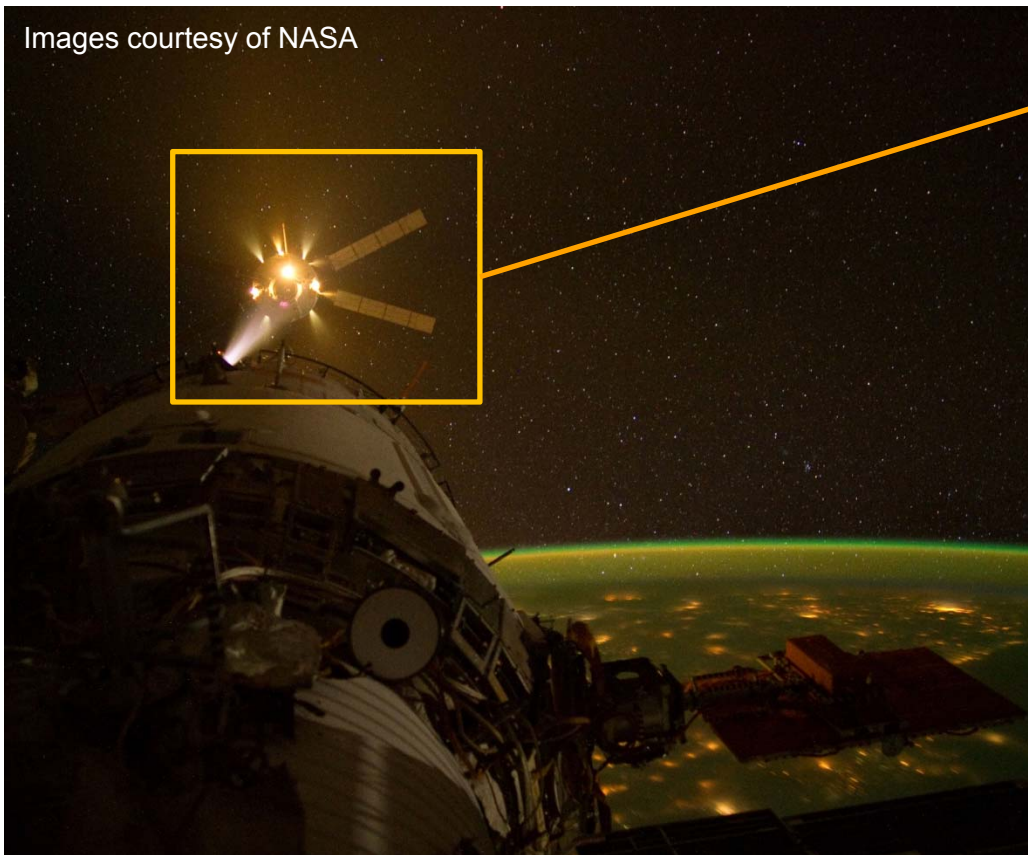




# Thruster Operations & Plume Effects

Engineering, Operations & Technology | Boeing Research & Technology

Images courtesy of NASA

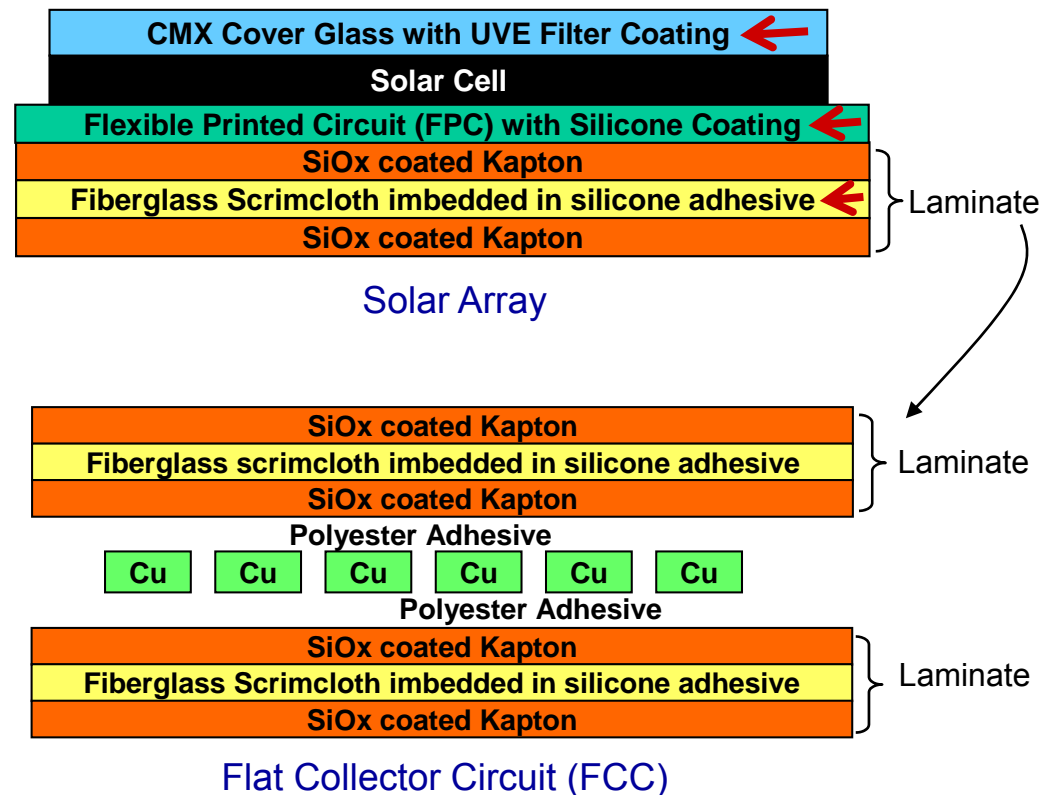


# Impacts to Optically Sensitive Surfaces

Engineering, Operations & Technology | Boeing Research & Technology

- **Thruster plume induced erosion of solar arrays**
  - Solar cell coverglass is damaged by droplet impacts. Damage impacts the performance of UVE filter coatings and increases optical scatter on the coverglass.
  - The laminates used on solar array thermal side can also be damaged. Thin silicon oxide (SiOx) coatings protect Kapton from Atomic Oxygen erosion.

## Representative Solar Array Construction

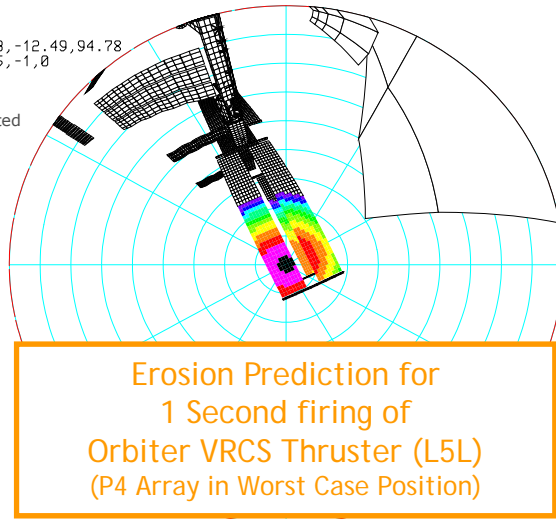
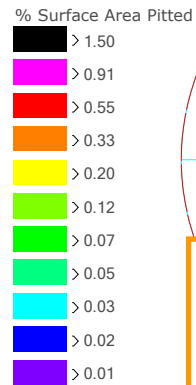


# Plume Induced Erosion Concerns

Engineering, Operations & Technology | Boeing Research & Technology

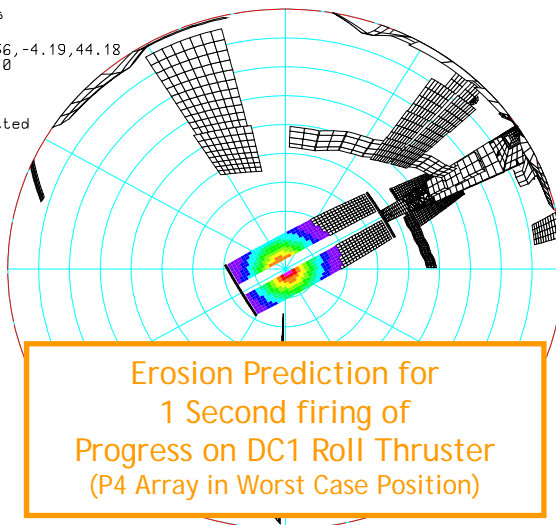
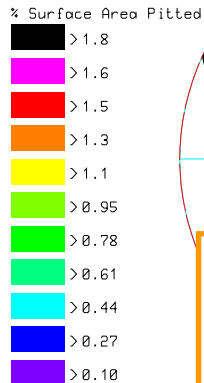
ORB L5L

Location : 29.93,-12.49,94.78  
Direction : 0.025,-1,0



Progress Thrusters  
PR11,12 & 25,26

Location : -77.56,-4.19,44.18  
Direction : 0,-1,0



## Erosion events of concern for the ISS solar arrays

- Soyuz/Progress approach and separation to Russian Segment docking ports
- Soyuz relocations
- Russian Segment reboost and attitude control
- Soyuz thruster tests
- Progress and Service Module thruster tests
- Commercial cargo transportation vehicles approach and separation
- Commercial crew transportation vehicles approach and separation
- *Orbiter approach and separation to PMA2*
- *Orbiter reboost and attitude control*





# ISS Solar Array Constraints

Engineering, Operations & Technology | Boeing Research & Technology

## Example of Current Erosion Constraint Table

### Service Module Roll/Pitch/Yaw Attitude Control - Inboard SAW Example

- Results for each alpha/beta combination represent maximum erosion on the entire solar array surface if that particular solar array alpha/beta combination is selected for every event within a year

		2A																																				
SARJ \ 2A	0	10	20	30	40	50	60	70	80	90	100	110	120	130	140	150	160	170	180	190	200	210	220	230	240	250	260	270	280	290	300	310	320	330	340	350		
0	###	###	###	8131	###	2261	432	0.00	0.00	0.00	68.2	359	1050	1920	###	6111	###	###	###	###	###	###	###	###	###	###	###	###	###	###	###	###	###	###	###	###	###	
15	###	###	1221	506	119	8.75	0.00	0.00	0.00	64.6	581	1525	###	###	7414	###	###	###	###	###	###	2410	1363	585	160	8.08	0.00	0.00	0.00	36.6	447	1276	3418	###	7410	7141	###	5651
30	###	###	1812	837	100	0.00	0.00	0.00	586	3126	###	###	###	###	###	###	###	###	###	###	###	1683	784	134	0.00	0.00	0.00	0.00	446	###	###	###	###	###	###	###	###	###
45	###	###	1641	265	0.00	0.00	0.00	26.4	638	1352	###	###	###	###	###	###	###	###	###	###	###	1712	334	0.00	0.00	0.00	7.22	645	1466	2177	3512	###	###	7021	7617	###	###	
60	855	492	129	0.00	0.00	0.00	0.00	21.7	65.9	167	314	654	1144	1646	###	2241	2134	1598	893	532	148	0.00	0.00	0.00	0.00	21.5	72.1	182	343	702	1229	1761	2173	###	2187	1587		
75	53.3	17.2	2.28	0.00	0.00	0.00	0.00	0.98	3.43	12.4	26.4	52.4	92.9	136	167	171	142	91.2	58.2	20.4	3.30	0.00	0.00	0.00	0.00	1.03	3.84	13.8	29.8	57.7	101	146	176	175	141	86.5		
90	1.46	0.44	0.02	0.00	0.00	0.00	0.00	0.02	0.12	0.40	1.09	1.98	3.60	4.95	5.97	5.85	4.51	3.27	1.67	0.52	0.03	0.00	0.00	0.00	0.00	0.00	0.03	0.14	0.44	1.23	2.17	3.84	5.28	6.19	5.86	4.33	3.08	
105	0.19	0.05	0.00	0.00	0.00	0.00	0.00	0.01	0.05	0.21	0.43	0.90	1.50	2.08	2.25	1.86	1.16	0.59	0.23	0.07	0.01	0.00	0.00	0.00	0.00	0.00	0.01	0.06	0.23	0.47	0.96	1.55	2.09	2.17	1.72	1.02	0.50	
120	0.08	0.02	0.00	0.00	0.00	0.00	0.00	0.00	0.02	0.07	0.20	0.33	0.55	0.71	0.75	0.63	0.43	0.22	0.10	0.03	0.00	0.00	0.00	0.00	0.00	0.00	0.00	0.02	0.08	0.21	0.34	0.55	0.69	0.70	0.57	0.37	0.18	
135	0.03	0.01	0.00	0.00	0.00	0.00	0.00	0.00	0.00	0.02	0.05	0.13	0.18	0.22	0.24	0.21	0.15	0.08	0.04	0.01	0.00	0.00	0.00	0.00	0.00	0.00	0.00	0.00	0.02	0.05	0.12	0.18	0.20	0.22	0.18	0.12	0.06	
150	0.01	0.00	0.00	0.00	0.00	0.00	0.00	0.00	0.00	0.00	0.00	0.02	0.05	0.08	0.09	0.07	0.06	0.04	0.02	0.01	0.00	0.00	0.00	0.00	0.00	0.00	0.00	0.00	0.00	0.00	0.00	0.00	0.00	0.00	0.00	0.00	0.00	0.00
165	0.01	0.00	0.00	0.00	0.00	0.00	0.00	0.00	0.00	0.00	0.00	0.00	0.00	0.01	0.02	0.02	0.02	0.02	0.01	0.01	0.00	0.00	0.00	0.00	0.00	0.00	0.00	0.00	0.00	0.00	0.00	0.00	0.00	0.00	0.00	0.00	0.00	0.00
180	0.01	0.01	0.02	0.02	0.01	0.01	0.00	0.00	0.00	0.00	0.00	0.00	0.00	0.00	0.00	0.00	0.00	0.01	0.01	0.02	0.02	0.02	0.02	0.02	0.01	0.00	0.00	0.00	0.00	0.00	0.00	0.00	0.00	0.00	0.00	0.00	0.00	0.00
195	0.02	0.04	0.06	0.08	0.09	0.07	0.04	0.02	0.00	0.00	0.00	0.00	0.00	0.00	0.00	0.00	0.00	0.01	0.03	0.05	0.08	0.10	0.10	0.08	0.04	0.02	0.00	0.00	0.00	0.00	0.00	0.00	0.00	0.00	0.00	0.00	0.00	0.00
210	0.06	0.11	0.19	0.26	0.29	0.27	0.24	0.14	0.05	0.01	0.00	0.00	0.00	0.00	0.00	0.00	0.00	0.03	0.08	0.13	0.22	0.30	0.32	0.29	0.26	0.14	0.05	0.01	0.00	0.00	0.00	0.00	0.00	0.00	0.00	0.00	0.00	0.00
225	0.15	0.34	0.65	0.95	1.12	1.06	0.80	0.48	0.29	0.09	0.02	0.00	0.00	0.00	0.00	0.00	0.01	0.06	0.19	0.41	0.74	1.05	1.19	1.09	0.80	0.46	0.27	0.08	0.02	0.00	0.00	0.00	0.00	0.00	0.00	0.00	0.00	0.00
240	0.39	1.03	2.01	3.19	3.83	3.54	2.56	1.57	0.72	0.35	0.08	0.00	0.00	0.00	0.00	0.00	0.03	0.16	0.48	1.22	2.25	3.42	3.94	3.52	2.45	1.46	0.66	0.32	0.07	0.00	0.00	0.00	0.00	0.00	0.00	0.00	0.00	
255	0.97	2.77	5.69	9.06	9.66	9.84	6.88	3.85	1.84	0.76	0.23	0.04	0.00	0.00	0.00	0.00	0.06	0.40	1.20	3.20	6.24	9.45	9.60	9.42	6.43	3.49	1.64	0.65	0.20	0.04	0.00	0.00	0.00	0.00	0.00	0.00		
270	2.19	6.01	12.2	16.4	13.6	15.3	13.2	7.21	3.34	1.28	0.42	0.08	0.00	0.00	0.00	0.00	0.15	0.91	2.67	6.86	13.2	16.7	13.4	14.5	12.2	6.48	2.94	1.09	0.36	0.07	0.00	0.00	0.00	0.00	0.00			
285	55.0	105	146	163	148	110	68.8	36.0	16.4	6.91	2.03	0.61	0.00	0.00	0.00	0.00	8.59	32.5	58.7	107	143	155	137	101	61.9	32.3	14.4	6.21	1.79	0.61	0.00	0.00	0.00	0.00	7.31	29.1		
300	906	1267	1422	1373	1129	808	516	298	195	103	43.1	0.09	0.00	0.00	0.00	55.1	261	483	893	1214	1344	1287	1054	754	480	275	142	92.5	39.8	0.33	0.00	0.00	0.00	43.3	241	483		
315	1340	1752	2167	###	2361	2413	2125	1605	882	472	67.0	0.00	0.00	0.00	64.4	310	491	845	1255	1646	###	2101	###	###	1997	1528	841	486	88.7	0.00	0.00	0.00	52.0	319	538	911		
330	###	5816	9501	###	###	###	1192	496	157	28.4	0.00	0.00	0.00	7.02	426	1273	###	###	###	###	###	4431	###	###	1288	531	200	26.4	0.00	0.00	6.77	332	1140	###	###			
345	###	###	8918	###	###	2811	1691	747	54.6	0.00	0.00	0.00	751	2681	###	###	###	###	###	###	###	###	###	###	###	###	###	###	###	###	###	###	###	###	###	###		
Interpolation Method	Maximum						Green_Min	0.00	Yellow_Min	0.10	Red_Min	1.00																										

NASA JSC 29181 Plume Model



# Original ISS Plume Erosion Model

Engineering, Operations & Technology | Boeing Research & Technology

- **Original liquid droplet distribution/flux model used by Space Environments was developed by NASA (JSC 29181)**

Reference: Larin, M.E., "Model For Predicting Liquid Droplet Distribution and Velocities In The Plumes Of Small Bipropellant Thrusters," JSC 29181, September 2000

- **Model was designed to determine feathering angles for ISS sensitive surfaces**
  - Quantifies liquid droplet distribution and velocities in the thruster plume through the analysis of the two-phase droplet-gas flow
- **Model was based on ground-based vacuum chamber data, and not correlated against light experiment data [SPIFEX, PIC]**
- **Space Environments' assessment of model predictions with SPIFEX flight experiment measurements demonstrated overestimation of droplet flux when compared to flight experiment data**
- **Plume erosion model was reassessed and updated to correlate with flight and high-speed impact test data**



# Plume Erosion Model

Engineering, Operations & Technology | Boeing Research & Technology

$$n(d, \theta) = \underbrace{\frac{D_0(T)}{S_m}}_{\text{Thruster term}} \cdot \underbrace{f_{nr}}_{\text{Range term}} \cdot \underbrace{\left(\frac{d}{d_{\min}}\right)^{-p}}_{\text{Size distribution term}} \cdot \underbrace{e^{-\frac{\theta^2}{2\sigma^2}}}_{\text{Angular distribution term}}$$

On centerline  $\theta = 0^\circ$  and term becomes unity

$\sigma$  is a function of  $d$  and contains droplet limiting angle information

- A value of 4.57 was determined for 'p' through an iterative procedure requiring a close match with droplet mass angular distribution results from a MBB 10 N thruster test by H. Trinks.
- Implementation by Space Environments of the droplet distribution model follows AIAA 2001-2816:

$$\dot{n}(T, d, r, \theta) = \underbrace{\frac{\dot{M}_T \cdot K \cdot T^{-\beta}}{S_m}}_{\text{Total propellant mass flow rate}} \cdot \underbrace{(r + l_{noz})^{-2}}_{\text{This is proportional to contaminant mass fraction (K, } \beta \text{ are constants)}} \cdot \underbrace{\left(\frac{d}{d_{\min}}\right)^{-4.57}}_{1/r^2 \text{ dependence}} \cdot e^{-\frac{\theta^2}{2\sigma^2}}$$

Droplet number flux

Reference: Soares et al., "International Space Station Bipropellant Plume Contamination Model," AIAA 2002-3016, June 2002





# Plume Contamination Model

Engineering, Operations & Technology | Boeing Research & Technology



- The plume erosion model uses the total liquid-phase contaminant flux from the plume contamination model (AIAA 2002-2016):

Contamination (e.g. g/cm<sup>2</sup>/s)

$$\dot{m}_C(r, \theta) = \underbrace{KT^{-\beta}}_{\text{“Contamination Ratio”}} \cdot \underbrace{\frac{\dot{M}_T}{R_{exit}^2}}_{\text{Thruster term}} \cdot \underbrace{\left(\frac{r + l_{noz}}{R_{exit}}\right)^{-2}}_{\text{Range term}} \cdot \underbrace{\left(2e^{\frac{\theta}{\theta_0}} - e^{-2\frac{\theta}{\theta_0}}\right)}_{\text{Angular distribution term}}$$

K and  $\beta$  are constants  
 1/r<sup>2</sup> dependence  
 On centerline  $\theta = 0^\circ$  and term becomes unity

- r is range (e.g. in cm)
- $\theta$  is angle off thruster plume centerline (degrees)
- T is thrust (N)
- $\dot{M}_T$  is the total propellant mass flow rate (e.g. in g/s)
- $R_{exit}$  is the nozzle exit radius (e.g. in cm; note this is just a reference distance)
- $l_{noz}$  is nozzle length (e.g. in cm)
- $\theta_0$  is the “dispersion coefficient” (5 degrees)

Reference: Soares et al., “International Space Station Bipropellant Plume Contamination Model,” AIAA 2002-3016, June 2002

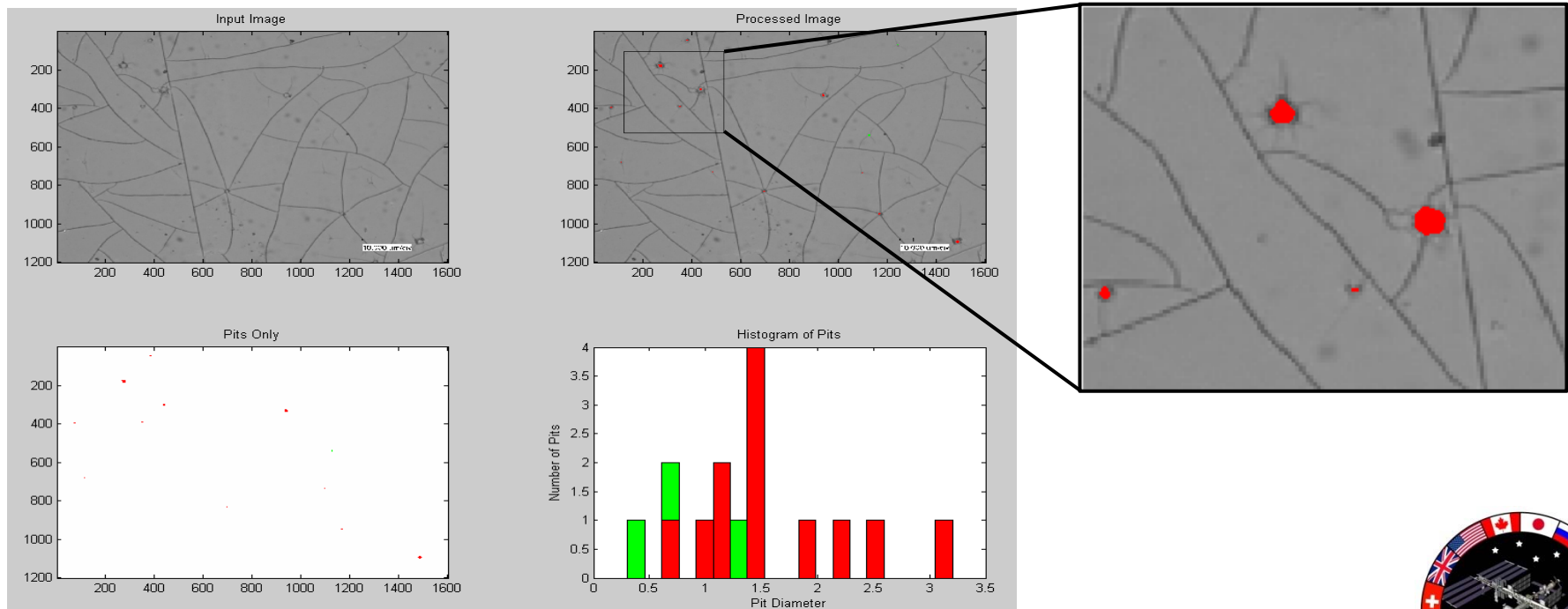


# Flight Experiment Data Pitsweeper Image Analysis



Engineering, Operations & Technology | Boeing Research & Technology

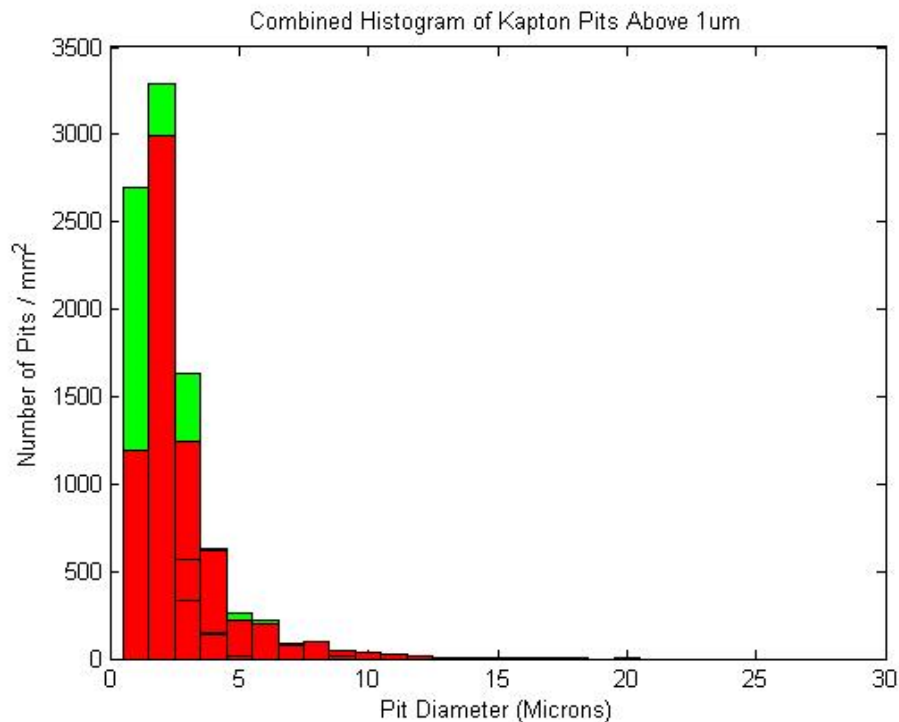
- Individual images were loaded into Pitsweeper image analysis program
- Pits were identified by user and separated into two groups
  - Pit (red bar)
  - Potential Pit (green bar)
- Pitsweeper outputed pit size distribution



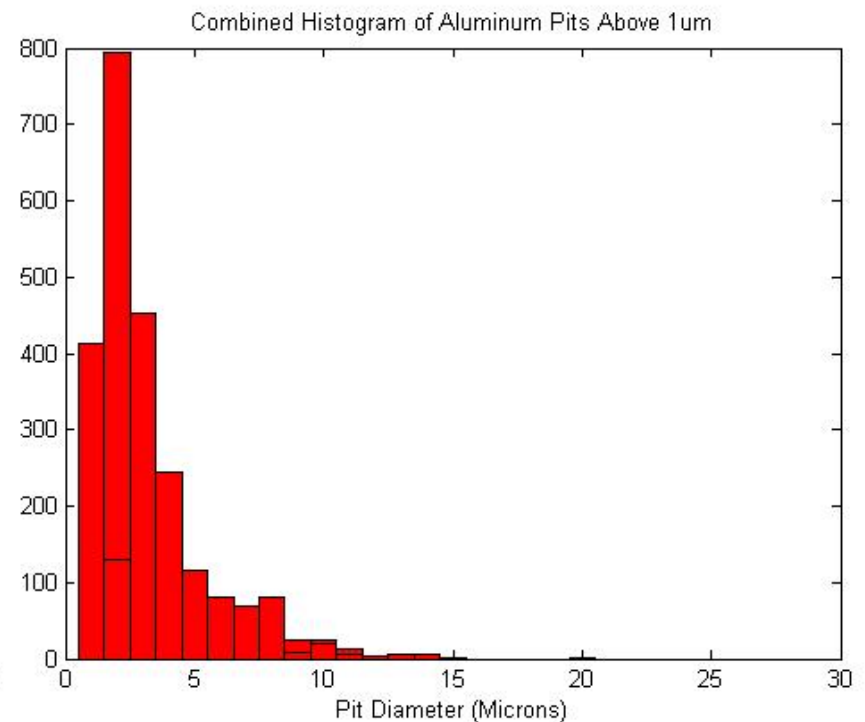
# Observed Erosion of SPIFEX Samples

Engineering, Operations & Technology | Boeing Research & Technology

## Kapton



## Aluminum



Green bars represent potential pits, or features in images of the samples suggestive of pits, but not well-resolved.

- **The Kapton and aluminum samples were adjacent in the experiment. Significant differences between the plots above indicate that surface material properties (i.e., hardness) has an important effect.**



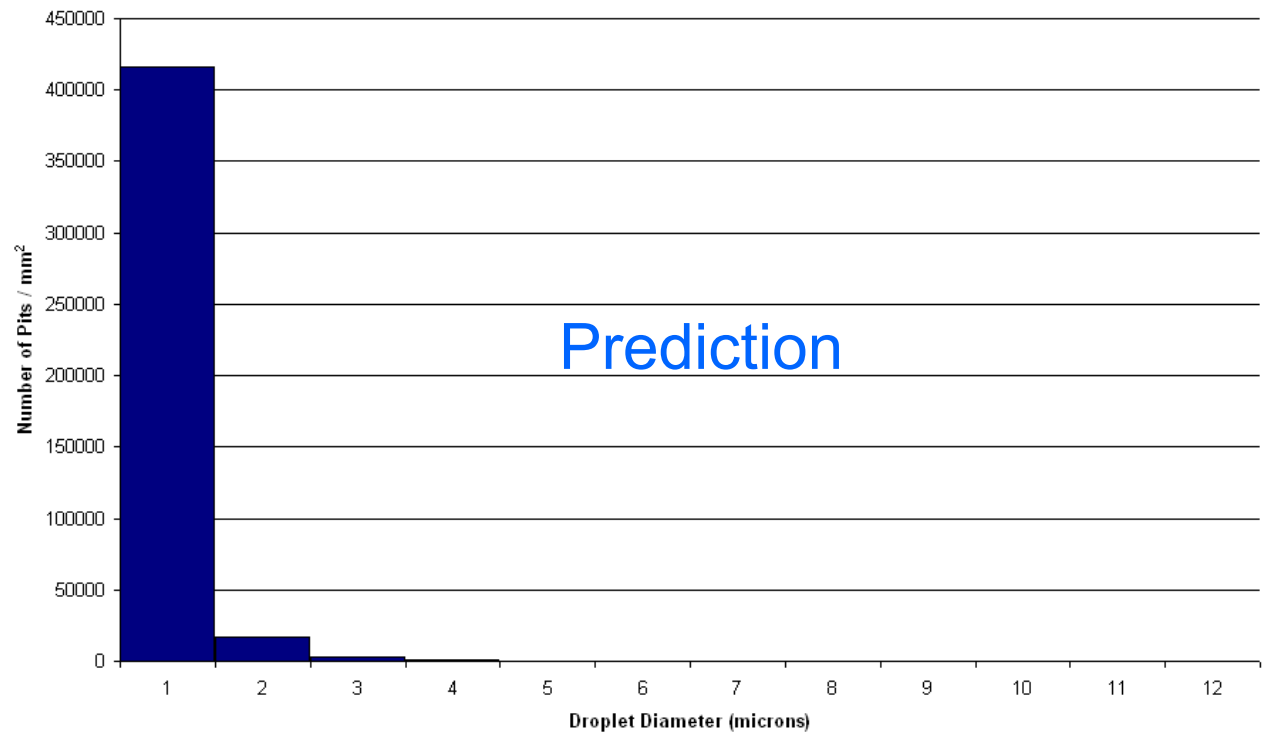
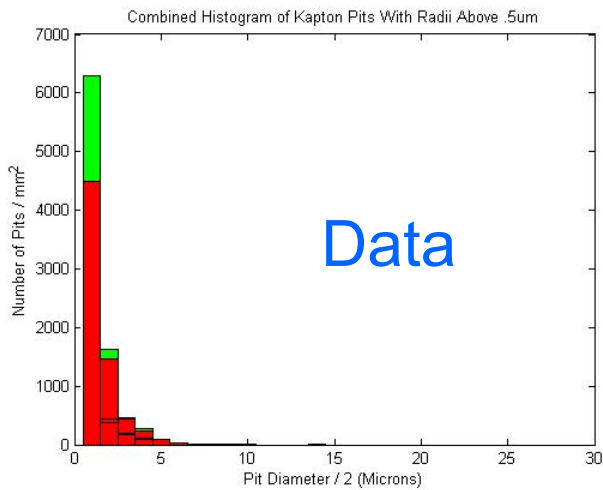
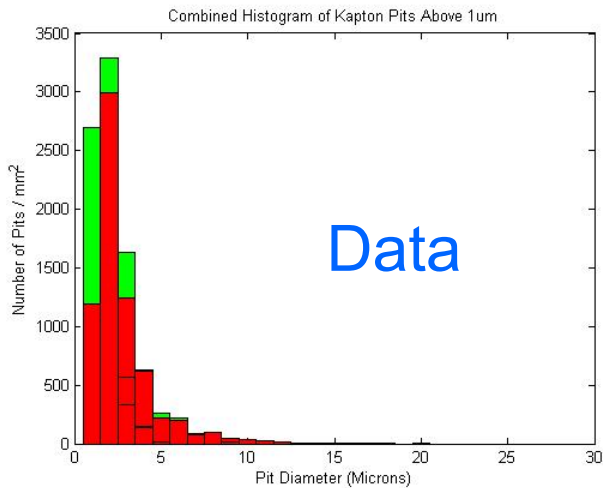
# Comparison of SPIFEX Kapton Pitting Fluences with Fluences Calculated with JSC 29181 Model

Engineering, Operations & Technology | Boeing Research & Technology



## JSC 29181 model assumptions

- Droplet size distribution coefficient:  $p = 4.57$  (controls particle size distribution)
- Maximum droplet diameter = 100  $\mu\text{m}$





# Update to Plume Erosion Model

Engineering, Operations & Technology | Boeing Research & Technology

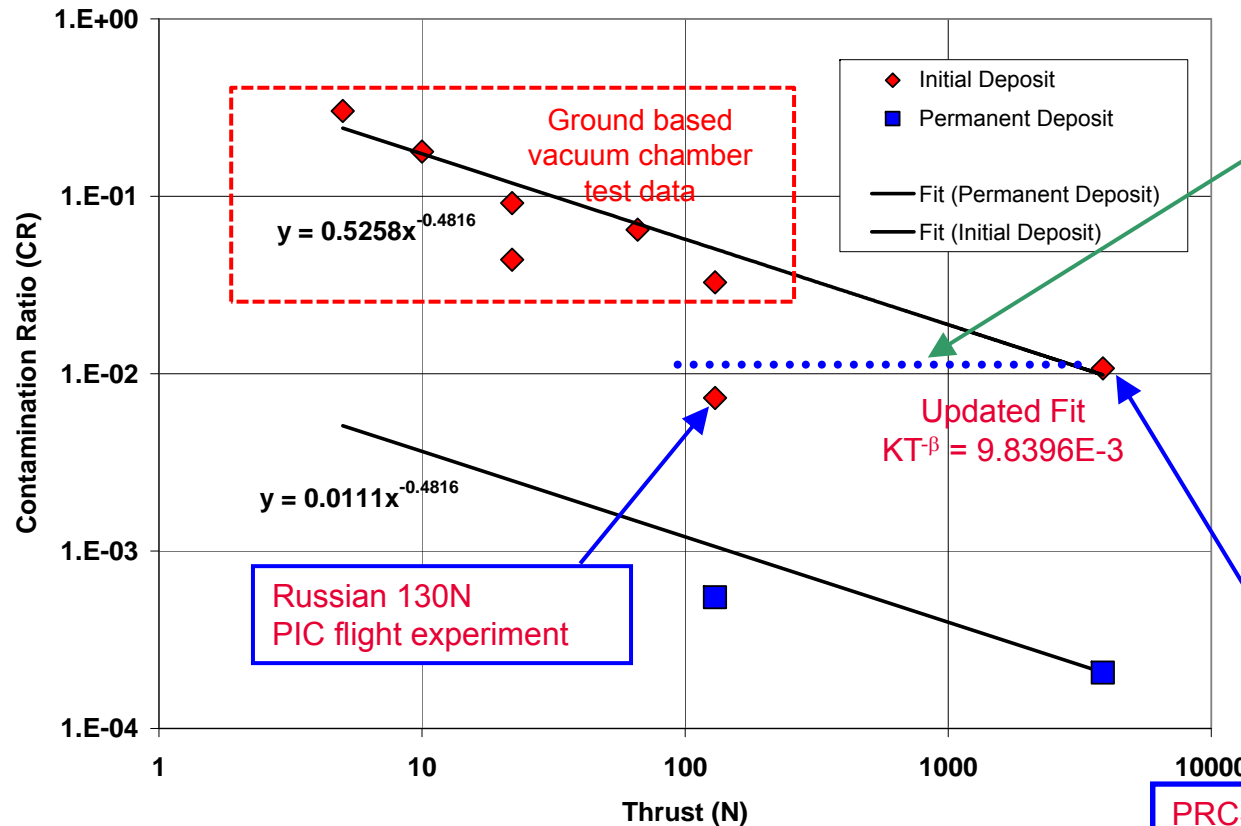
- **JSC 29181 plume model assumes a maximum droplet diameter of 100  $\mu\text{m}$**
- **Flight experiment measurements support a maximum droplet size of 12 to 24  $\mu\text{m}$  (based on calculations showing that droplets produce pits one to two times their diameter):**
  - Top five pit diameters ( $\mu\text{m}$ ) on SPIFEX samples:
    - Kapton: 20.3, 19.7, 18.4, 17.9, 17.4
    - Aluminum: 19.8, 15.5, 15.5, 15.5, 15.3
  - Largest pit diameter ( $\mu\text{m}$ ) reported for PIC experiment: 24
- **Boeing Space Environments conducted a parametric study and arrived at an updated plume model producing good correlation with the SPIFEX Kapton data. This was achieved by lowering the maximum droplet size and adjusting the droplet size distribution coefficient  $p$**



# Initial Contaminant Flux

Engineering, Operations & Technology | Boeing Research & Technology

- For the thrust level of interest (100-3870N), the contamination ratio ( $KT^{-\beta}$ ) was revised to fit the on-orbit data from the PIC flight experiment.



- $KT^{-\beta}$  becomes independent of thrust and is a constant:

$$0.5258 * 3870^{-0.4816} = 9.8396E-3$$

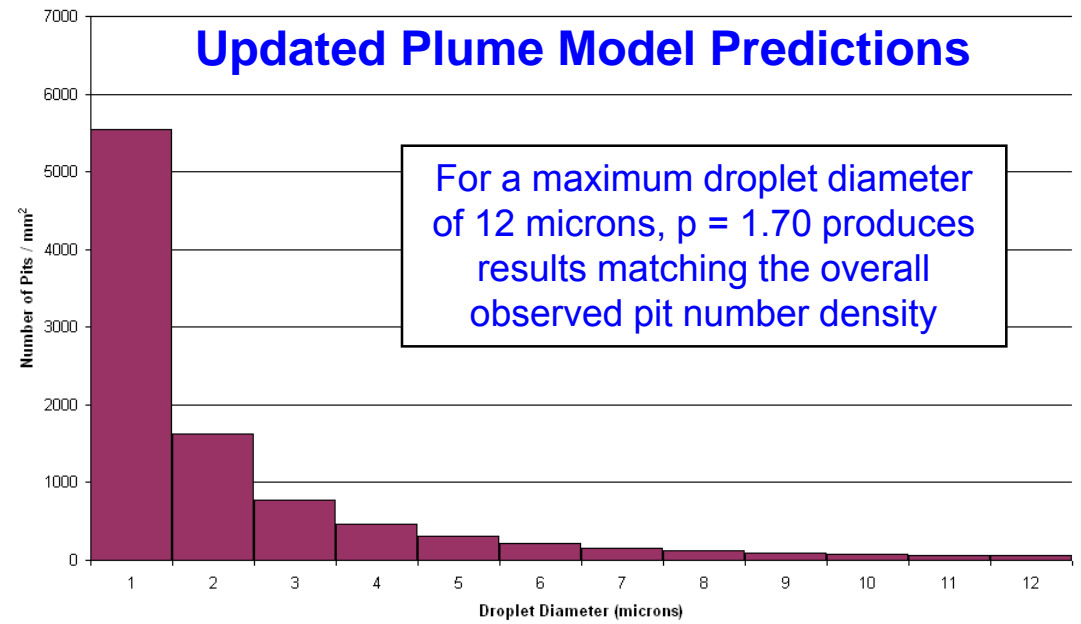
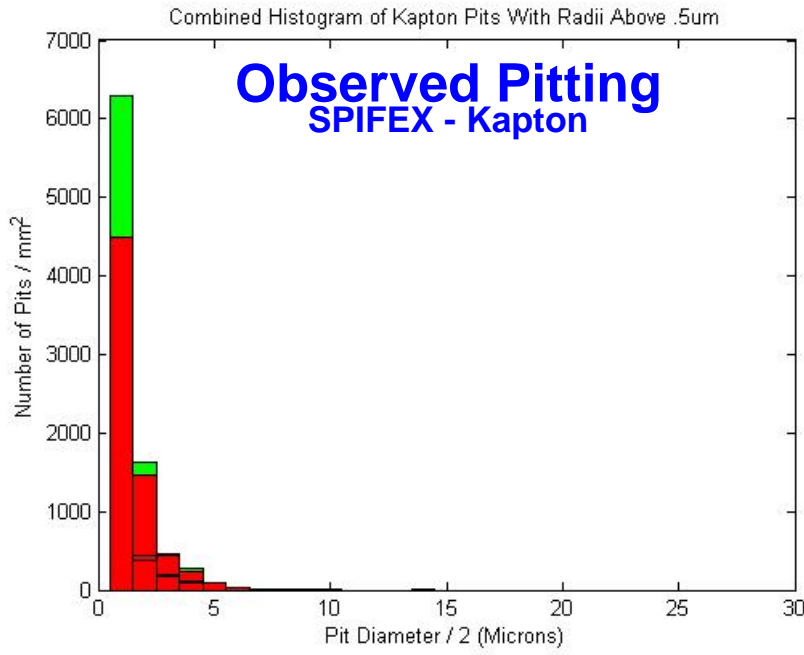
- Contaminant mass is predicted to be less than 2% of total propellant mass
- Reduction achieves factor of 5-6 reduction in initial deposition estimates

PRCS (3870 N) result from PIC flight experiment



# Comparison of SPIFEX Flight Experiment Data with Boeing Space Environments' Updated Plume Model

Engineering, Operations & Technology | Boeing Research & Technology



Updated Boeing Plume Model

## Model assumptions/notes

- Droplet size distribution coefficient:  $p = 1.70$
  - The maximum droplet diameter is  $12 \mu\text{m}$
- Requires 1:2 droplet-to-pit size assumption (allows pits up to  $24 \mu\text{m}$ , as reported for the PIC flight experiment)
- 1:1 droplet-to-pit ratio did not correlate



# Summary of Boeing Space Environments' Plume Model Update



Engineering, Operations & Technology | Boeing Research & Technology

- **Simulations of SPIFEX Kapton pitting levels with the JSC 29181 plume erosion model demonstrated that model needed to be updated**
- **Boeing Space Environments' plume model update correlates well with observed SPIFEX Kapton pitting results when:**
  - Maximum droplet diameter changed from 100  $\mu\text{m}$  to 12  $\mu\text{m}$  based on observed maximum pit diameters (and based on 1:2 relationship of droplet diameter to pit diameter)
  - Droplet limiting angle calculation updated per input from NASA JSC Aerosciences
  - Droplet size distribution coefficient " $p$ " (which controls particle size distribution) changed from 4.57 to 1.70





# Returned Node 1 Nadir Window Hyzod Cover



Engineering, Operations & Technology | Boeing Research & Technology

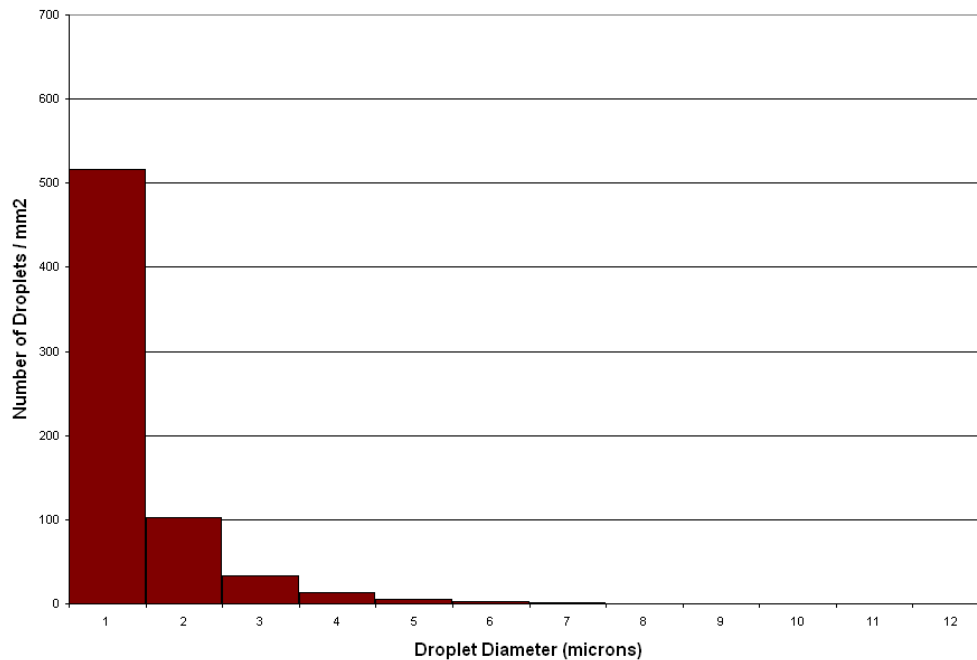
- **Node 1 nadir window Hyzod cover was deployed on ISS from Flight UF2 (June 2002) to Flight LF1 (July 2005) during which it was exposed to thruster firings for various Soyuz and Progress proximity operation events (approaches and separations of vehicles)**
- **NASA JSC Materials Evaluation Laboratory performed a microscopy imaging survey on the returned Hyzod material. Image survey results were delivered to the Space Environments Team for analysis**
- **Boeing Space Environments team developed an image analysis technique for this study to measure the damage crater sizes and performed the analysis**
  - Top five impact feature (pit) diameters ( $\mu\text{m}$ ): 16.6, 13.5, 7.5, 7.4, 7.3



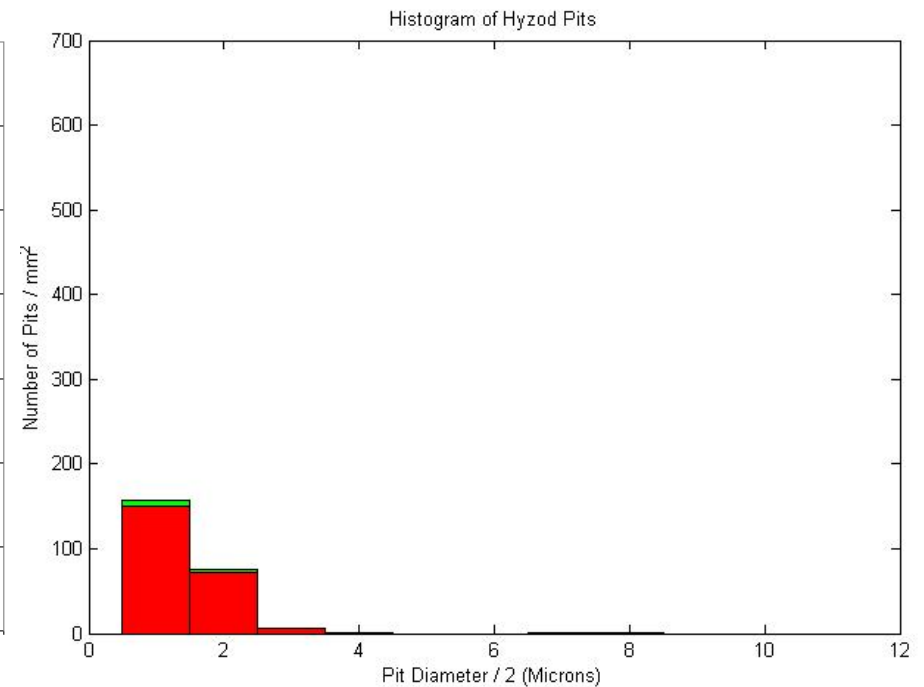
# Comparison Between Observed Hyzod Pitting Levels with Boeing Updated Plume Model Calculations

Engineering, Operations & Technology | Boeing Research & Technology

## Incident Droplet Fluence



## Observed Pitting



- Hyzod, as well as aluminum, which are harder materials than Kapton, demonstrate lower pit damage than Kapton which is a softer material



# Ground Testing & Analyses

Engineering, Operations & Technology | Boeing Research & Technology

- **Hypervelocity Impact (HVI) tests supported of reduction of solar array constraints from thruster plume induced erosion**
  - HVI test program was conducted by the NASA JSC Hypervelocity Impact Technology Facility (HITF)
    - Light gas gun testing conducted at the NASA JSC White Sands Test Facility (WSTF)
  - Detailed test objectives:
    - Address impact craters as a function of particle size, particle velocity and impacted material
    - Define calibration data for SPHINX
    - Assess solar cell power collection degradation as a function of surface damage
    - Assess scrim cloth mechanical damage due to particle impacts

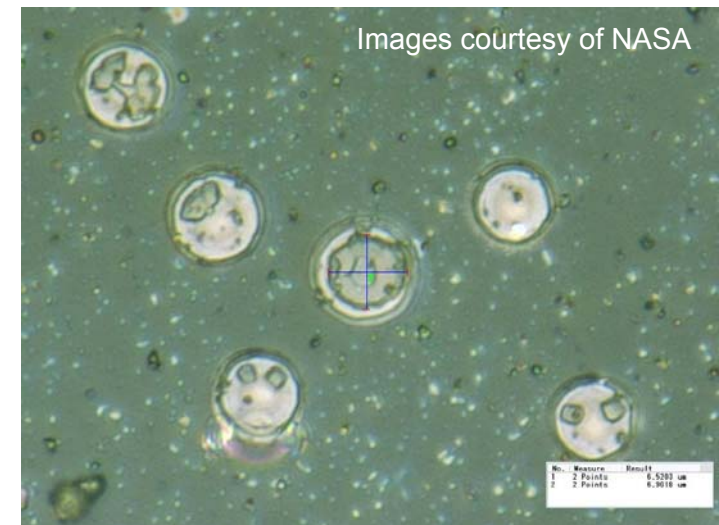


# Summary of Ground-Based Light Gas Gun Test Results



Engineering, Operations & Technology | Boeing Research & Technology

- High-speed impact testing (using a light gas gun system) was performed at the NASA WSTF on Hyzod, solar cell, and scrim cloth samples
- Optical microscopic imaging was performed on the samples at the HITF prior to and after the samples were shot with the light gas gun
- The core damage diameter was estimated from the test samples images
- Results show that the ratio of the core damage diameter/projectile diameter was less than 2.0 for the samples that were tested (Hyzod, solar cell, calibration samples)
  - SPHINX analysis results confirm core damage diameter / projectile diameter less than 2.0 for plume droplet impacts



Example Solar Cell Ground Test Image  
5 micron impacting at 1.82 km/s  
HITF08212 Post Test image (5000X)







# Application of Methodology (concluded)

Engineering, Operations & Technology | Boeing Research & Technology



## 2A

SARJ \ 2A	0	10	20	30	40	50	60	70	80	90	100	110	120	130	140	150	160	170	180	190	200	210	220	230	240	250	260	270	280	290	300	310	320	330	340	350			
0	###	###	###	###	###	###	###	###	###	###	###	###	###	###	###	###	###	###	###	###	###	###	###	###	###	###	###	###	###	###	###	###	###	###	###	###	###	###	
15	###	###	###	###	###	###	###	###	###	###	###	###	###	###	###	###	###	###	###	###	###	###	###	###	###	###	###	###	###	###	###	###	###	###	###	###	###	###	
30	###	###	###	###	###	###	###	###	###	###	###	###	###	###	###	###	###	###	###	###	###	###	###	###	###	###	###	###	###	###	###	###	###	###	###	###	###	###	
45	###	###	###	###	###	###	###	###	###	###	###	###	###	###	###	###	###	###	###	###	###	###	###	###	###	###	###	###	###	###	###	###	###	###	###	###	###	###	
60	###	###	###	###	###	###	###	###	###	###	###	###	###	###	###	###	###	###	###	###	###	###	###	###	###	###	###	###	###	###	###	###	###	###	###	###	###	###	
75	###	###	###	###	###	###	###	###	###	###	###	###	###	###	###	###	###	###	###	###	###	###	###	###	###	###	###	###	###	###	###	###	###	###	###	###	###	###	
90	###	###	###	###	###	###	###	###	###	###	###	###	###	###	###	###	###	###	###	###	###	###	###	###	###	###	###	###	###	###	###	###	###	###	###	###	###	###	
105	###	###	###	###	###	###	###	###	###	###	###	###	###	###	###	###	###	###	###	###	###	###	###	###	###	###	###	###	###	###	###	###	###	###	###	###	###	###	
120	###	###	###	###	###	###	###	###	###	###	###	###	###	###	###	###	###	###	###	###	###	###	###	###	###	###	###	###	###	###	###	###	###	###	###	###	###	###	
135	###	###	###	###	###	###	###	###	###	###	###	###	###	###	###	###	###	###	###	###	###	###	###	###	###	###	###	###	###	###	###	###	###	###	###	###	###	###	
150	###	###	###	###	###	###	###	###	###	###	###	###	###	###	###	###	###	###	###	###	###	###	###	###	###	###	###	###	###	###	###	###	###	###	###	###	###	###	
165	###	###	###	###	###	###	###	###	###	###	###	###	###	###	###	###	###	###	###	###	###	###	###	###	###	###	###	###	###	###	###	###	###	###	###	###	###	###	
180	###	###	###	###	###	###	###	###	###	###	###	###	###	###	###	###	###	###	###	###	###	###	###	###	###	###	###	###	###	###	###	###	###	###	###	###	###	###	
195	###	###	###	###	###	###	###	###	###	###	###	###	###	###	###	###	###	###	###	###	###	###	###	###	###	###	###	###	###	###	###	###	###	###	###	###	###	###	###
210	###	###	###	###	###	###	###	###	###	###	###	###	###	###	###	###	###	###	###	###	###	###	###	###	###	###	###	###	###	###	###	###	###	###	###	###	###	###	
225	###	###	###	###	###	###	###	###	###	###	###	###	###	###	###	###	###	###	###	###	###	###	###	###	###	###	###	###	###	###	###	###	###	###	###	###	###	###	
240	###	###	###	###	###	###	###	###	###	###	###	###	###	###	###	###	###	###	###	###	###	###	###	###	###	###	###	###	###	###	###	###	###	###	###	###	###	###	
255	###	###	###	###	###	###	###	###	###	###	###	###	###	###	###	###	###	###	###	###	###	###	###	###	###	###	###	###	###	###	###	###	###	###	###	###	###	###	###
270	###	###	###	###	###	###	###	###	###	###	###	###	###	###	###	###	###	###	###	###	###	###	###	###	###	###	###	###	###	###	###	###	###	###	###	###	###	###	###
285	###	###	###	###	###	###	###	###	###	###	###	###	###	###	###	###	###	###	###	###	###	###	###	###	###	###	###	###	###	###	###	###	###	###	###	###	###	###	###
300	###	###	###	###	###	###	###	###	###	###	###	###	###	###	###	###	###	###	###	###	###	###	###	###	###	###	###	###	###	###	###	###	###	###	###	###	###	###	###
315	###	###	###	###	###	###	###	###	###	###	###	###	###	###	###	###	###	###	###	###	###	###	###	###	###	###	###	###	###	###	###	###	###	###	###	###	###	###	###
330	###	###	###	###	###	###	###	###	###	###	###	###	###	###	###	###	###	###	###	###	###	###	###	###	###	###	###	###	###	###	###	###	###	###	###	###	###	###	###
345	###	###	###	###	###	###	###	###	###	###	###	###	###	###	###	###	###	###	###	###	###	###	###	###	###	###	###	###	###	###	###	###	###	###	###	###	###	###	###
Interpolation Method	Maximum					Green Min					0.00					Yellow Min					0.10					Red Min					1.00								

JSC 29181 Plume Model

Soyuz/Progress FGB Nadir Approach & SM RPY Attitude Control Port Inboard SAW

## 2A

SARJ \ 2A	0	10	20	30	40	50	60	70	80	90	100	110	120	130	140	150	160	170	180	190	200	210	220	230	240	250	260	270	280	290	300	310	320	330	340	350	
0	1381	1336	1234	1006	607	284	46.5	0.21	0.31	0.36	2.13	26.3	104	264	451	729	961	1157	1339	1298	1198	994	636	329	66.8	0.20	0.30	0.35	1.80	27.1	109	277	469	749	985	1190	
15	88.6	71.4	35.2	13.1	2.92	0.07	0.10	0.19	0.31	0.39	11.1	29.2	76.9	109	124	147	119	103	92.6	78.6	42.3	16.5	4.24	0.07	0.09	0.18	0.29	0.52	8.05	23.2	66.4	101	121	151	126	103	
30	212	106	61.2	23.0	2.89	0.02	0.07	0.14	0.20	0.77	317	540	616	584	590	490	383	316	198	98.6	96.0	20.7	3.59	0.02	0.07	0.13	0.22	0.58	309	551	651	623	629	511	409	337	
45	212	138	77.8	12.3	0.00	0.00	0.03	0.74	20.0	37.2	54.1	88.2	128	144	160	180	203	231	199	131	80.0	15.6	1.00	0.00	0.02	0.13	0.15	0.17	59.5	95.8	139	156	174	196	222	252	
60	18.6	11.1	2.73	0.00	0.00	0.00	0.00	0.28	0.97	2.72	5.14	11.1	20.2	27.7	33.9	39.7	43.9	34.1	19.6	12.1	3.29	0.00	0.00	0.00	0.00	0.29	1.09	3.04	5.78	12.2	22.3	30.6	36.9	42.3	45.7	33.9	
75	0.56	0.20	0.02	0.00	0.00	0.00	0.00	0.00	0.02	0.11	0.23	0.48	0.88	1.34	1.69	1.77	1.50	0.97	0.62	0.24	0.03	0.00	0.00	0.00	0.00	0.00	0.00	0.03	0.13	0.27	0.54	0.98	1.46	1.86	1.82	1.48	0.91
90	0.00	0.00	0.00	0.00	0.00	0.00	0.00	0.00	0.00	0.00	0.01	0.01	0.02	0.03	0.03	0.02	0.01	0.01	0.00	0.00	0.00	0.00	0.00	0.00	0.00	0.00	0.00	0.00	0.01	0.02	0.03	0.03	0.03	0.02	0.01	0.01	
105	0.00	0.00	0.00	0.00	0.00	0.00	0.00	0.00	0.00	0.00	0.00	0.00	0.00	0.00	0.00	0.00	0.00	0.00	0.00	0.00	0.00	0.00	0.00	0.00	0.00	0.00	0.00	0.00	0.00	0.00	0.00	0.00	0.00	0.00	0.00	0.00	0.00
120	0.00	0.00	0.02	0.04	0.05	0.06	0.06	0.05	0.03	0.01	0.00	0.00	0.00	0.00	0.00	0.00	0.00	0.00	0.00	0.02	0.04	0.05	0.06	0.06	0.05	0.03	0.01	0.00	0.00	0.00	0.00	0.00	0.00	0.00	0.00	0.00	0.00
135	0.00	0.01	0.06	0.11	0.18	0.23	0.27	0.27	0.24	0.18	0.11	0.05	0.01	0.00	0.00	0.00	0.00	0.01	0.05	0.10	0.17	0.23	0.26	0.27	0.24	0.19	0.12	0.05	0.01	0.00	0.00	0.00	0.00	0.00	0.00	0.00	0.00
150	0.01	0.03	0.09	0.20	0.31	0.41	0.51	0.55	0.52	0.44	0.34	0.23	0.10	0.03	0.00	0.00	0.00	0.01	0.03	0.03	0.20	0.30	0.40	0.50	0.54	0.52	0.45	0.35	0.24	0.11	0.03	0.00	0.00	0.00	0.00	0.00	0.00
165	0.02	0.05	0.13	0.27	0.44	0.65	0.81	0.88	0.87	0.78	0.60	0.39	0.23	0.09	0.01	0.00	0.01	0.01	0.02	0.05	0.12	0.26	0.43	0.63	0.79	0.87	0.87	0.78	0.61	0.40	0.24	0.09	0.01	0.00	0.00	0.00	0.00
180	0.10	0.15	0.20	0.30	0.54	0.76	0.92	1.08	1.10	0.95	0.77	0.52	0.29	0.13	0.02	0.02	0.04	0.07	0.11	0.15	0.19	0.29	0.52	0.74	0.90	1.07	1.10	0.96	0.79	0.54	0.30	0.14	0.03	0.01	0.04	0.06	
195	0.65	0.83	0.90	0.83	0.70	0.75	0.94	1.19	1.18	0.95	0.75	0.53	0.29	0.14	0.03	0.00	0.29	0.45	0.67	0.83	0.88	0.79	0.65	0.73	0.92	1.17	1.15	0.96	0.79	0.54	0.30	0.14	0.03	0.01	0.04	0.06	
210	2.16	2.57	2.68	2.49	2.12	1.61	1.14	0.91	0.87	0.79	0.63	0.40	0.23	0.09	0.05	0.41	1.08	1.56	2.10	2.52	2.62	2.44	2.07	1.57	1.10	0.83	0.66	0.80	0.64	0.41	0.24	0.10	0.03	0.06	1.03	1.54	
225	2.31	2.98	3.25	3.29	3.11	2.77	2.27	1.66	1.22	0.77	0.35	0.24	0.12	0.03	0.10	0.48	1.07	1.56	2.27	2.89	3.17	3.24	3.07	2.67	2.18	1.59	1.17	0.76	0.37	0.25	0.13	0.04	0.09	0.50	1.11</		

# Conclusions

Engineering, Operations & Technology | Boeing Research & Technology

- **This paper presents the methodology employed in updating the ISS plume induced erosion model for better correlation with flight experiment data and for increased accuracy**
- **The plume induced erosion model originally developed to support the Program significantly over-predicted erosion damage**
- **Boeing Space Environments succeeded in adjusting the model for better correlation with flight experiment results**
- **The updated plume model was successfully applied in the definition of updated constraints for ISS solar array operations while mitigating against excessive erosion to the arrays. Erosion keep-out zones for ISS solar arrays were reduced by 30% to 60% with the updated model**
- **The authors hope that future efforts to improve the characterization of plume induced erosion will draw upon the expertise developed for the ISS Program in the development of space environments effects modeling**



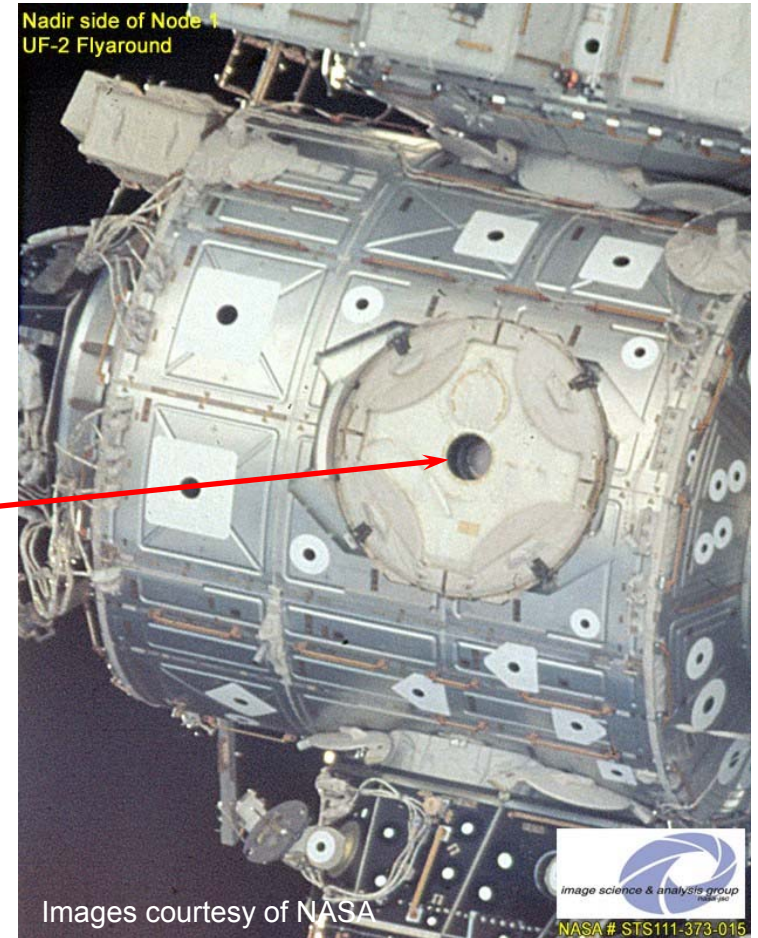
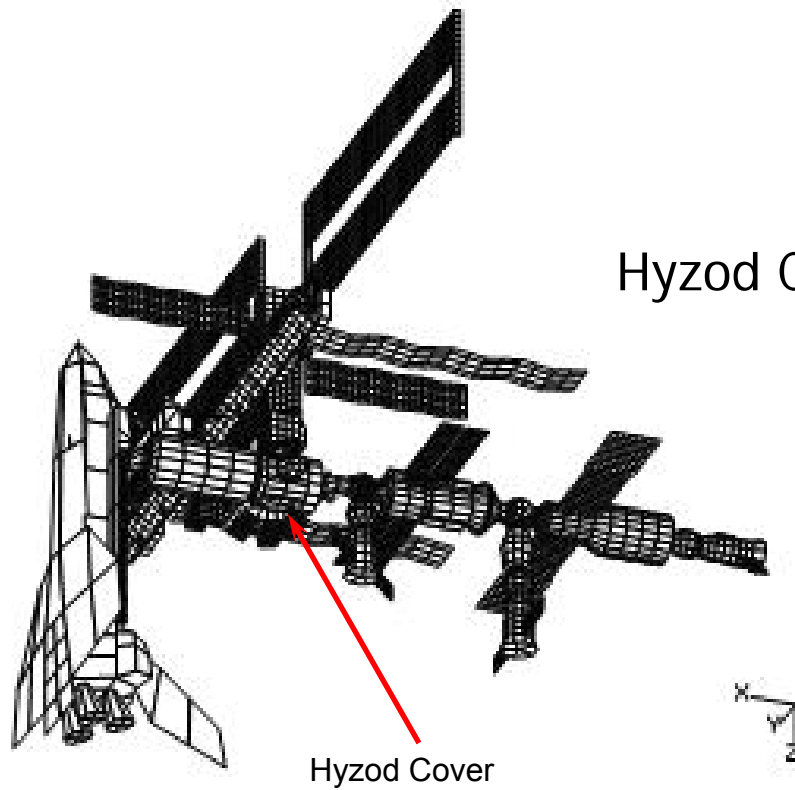
# Backup



# Hyzod Window Cover Background

Engineering, Operations & Technology | Boeing Research & Technology

- Node 1 nadir window cover
- Exposed from June 2002 (STS-111/UF2) to July 2005 (STS-114/LF1)





# Hyzod Exposures to Thruster Plumes

Engineering, Operations & Technology | Boeing Research & Technology

- Hyzod window cover exposed to thruster firings during Orbiter, Soyuz, and Progress Proximity Operations

Thruster	Docking Port	Number of Approaches	Number of Separations
Orbiter	PMA2	3	3
Soyuz*	FGB	4	4
Soyuz	DC1	4	4
Progress	DC1	1	1
Progress	SM Aft	10	10

\* Expected to be the dominant source of plume effects



# Example Hyzod Image (1000x Magnification)

Engineering, Operations & Technology | Boeing Research & Technology



# Summary of Hyzod Image Analysis Results

Engineering, Operations & Technology | Boeing Research & Technology

- **Most common pit size is 2 – 3  $\mu\text{m}$  for both magnification levels**
- **Largest pit diameter is approximately 17  $\mu\text{m}$**
- **99.8% of pits are below 8  $\mu\text{m}$**
- **Pits with diameters less than 1  $\mu\text{m}$  are visible in 3000x images but not in 1000x images**
- **Number densities inferred from the 3000x images are up to two times larger than the 1000x images**

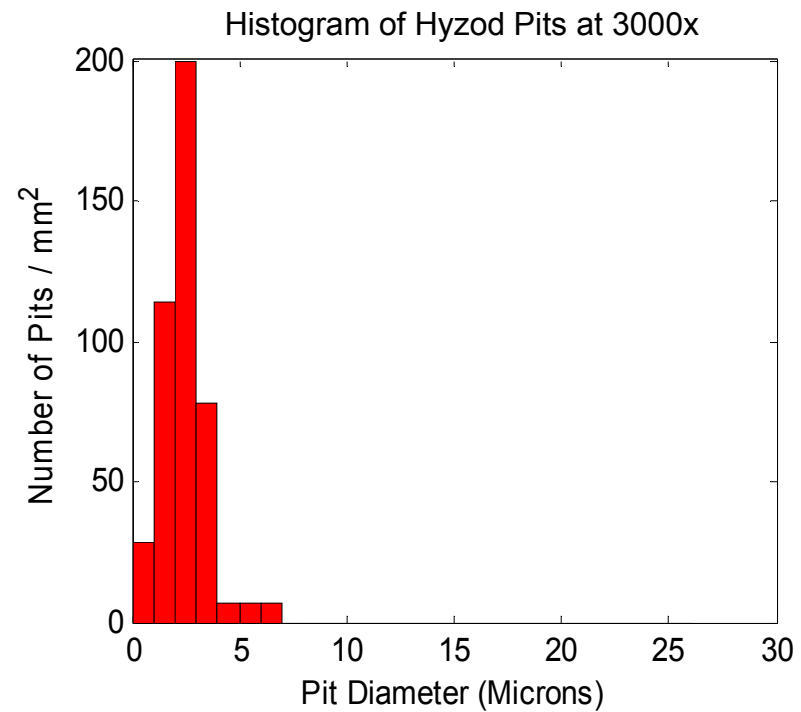
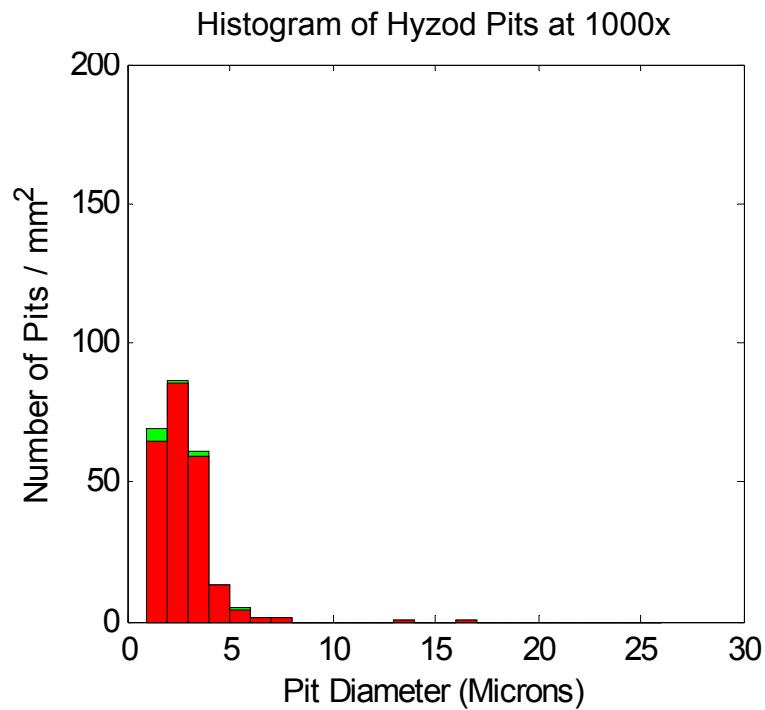


# Hyzod Image Analysis Results

Engineering, Operations & Technology | Boeing Research & Technology

90 Images  
5.7 mm<sup>2</sup>

20 Images  
0.2 mm<sup>2</sup>



Note: Histograms show normalized pit size distributions

Note: 3000x magnification images provided only for comparison purposes. Image samples insufficient for quantitative assessment



# Hyzod Image Analysis Results

Engineering, Operations & Technology | Boeing Research & Technology



Magnification	Approximate Pit Number Density Excluding Potential Pits (pits / mm <sup>2</sup> )	Approximate Pit Number Density Including Potential Pits (pits / mm <sup>2</sup> )
1000x	230	240
3000x	410	410

Note: Pit density rounded to the nearest multiple of ten pits / mm<sup>2</sup>

Magnification	Approximate % Total Area Pitted Excluding Potential Pits	Approximate % Total Area Pitted Including Potential Pits
1000x	0.16 %	0.16 %
3000x	0.24%	0.24%

Note: 3000x magnification images provided only for comparison purposes. Image samples insufficient for quantitative assessment





# SPIFEX Background

Engineering, Operations & Technology | Boeing Research & Technology



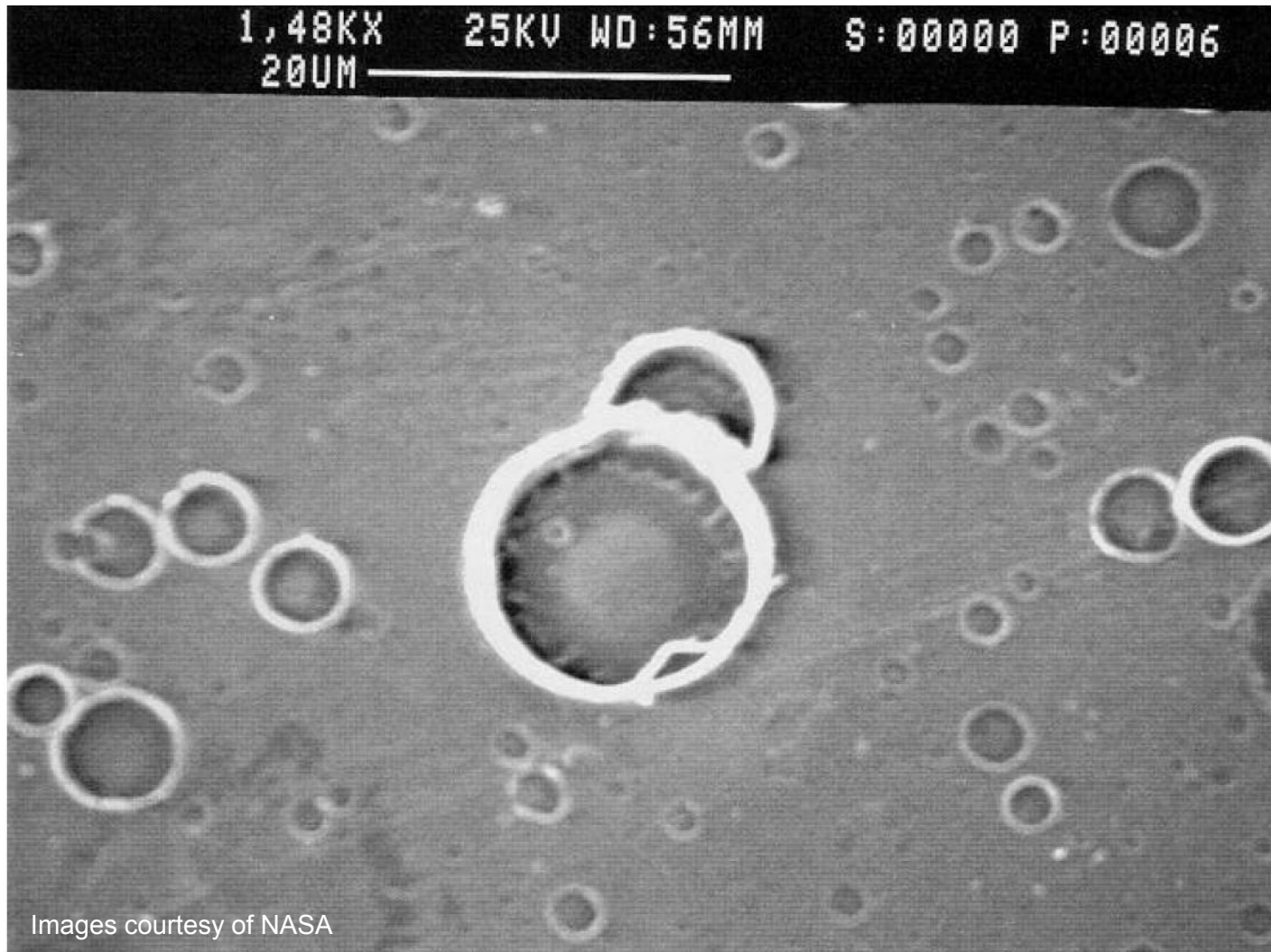
- **Experiment conducted by the U.S. in September 1994 (STS-64)**
- **Exposed samples of Kapton tape and aluminum foil to:**
  - 84 PRCS firings
  - 17 VRCS firings
  - Average pulse of 248.5 ms
  - Average distance of 46 feet
  - Angles off centerline varied from 0° to 90°
- **Of interest to compare results for Kapton tape and aluminum foil to evaluate differences in material susceptibility to impact damage**



# Example SPIFEX Kapton Tape Image: 1500x Magnification (20 $\mu\text{m}$ Scale)

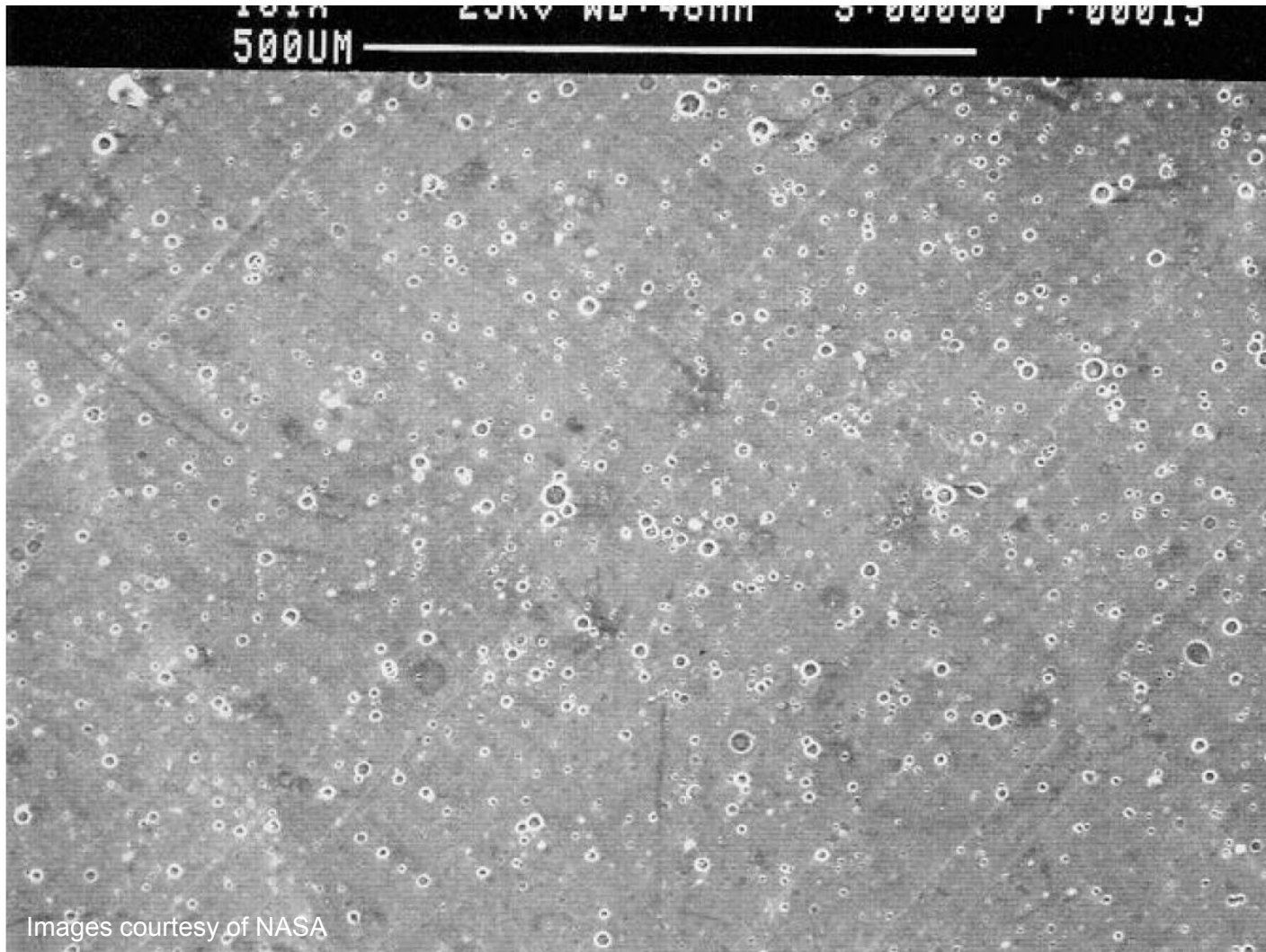


Engineering, Operations & Technology | Boeing Research & Technology



# Example SPIFEX Kapton Tape Image: 100x Magnification (500 $\mu\text{m}$ Scale)

Engineering, Operations & Technology | Boeing Research & Technology

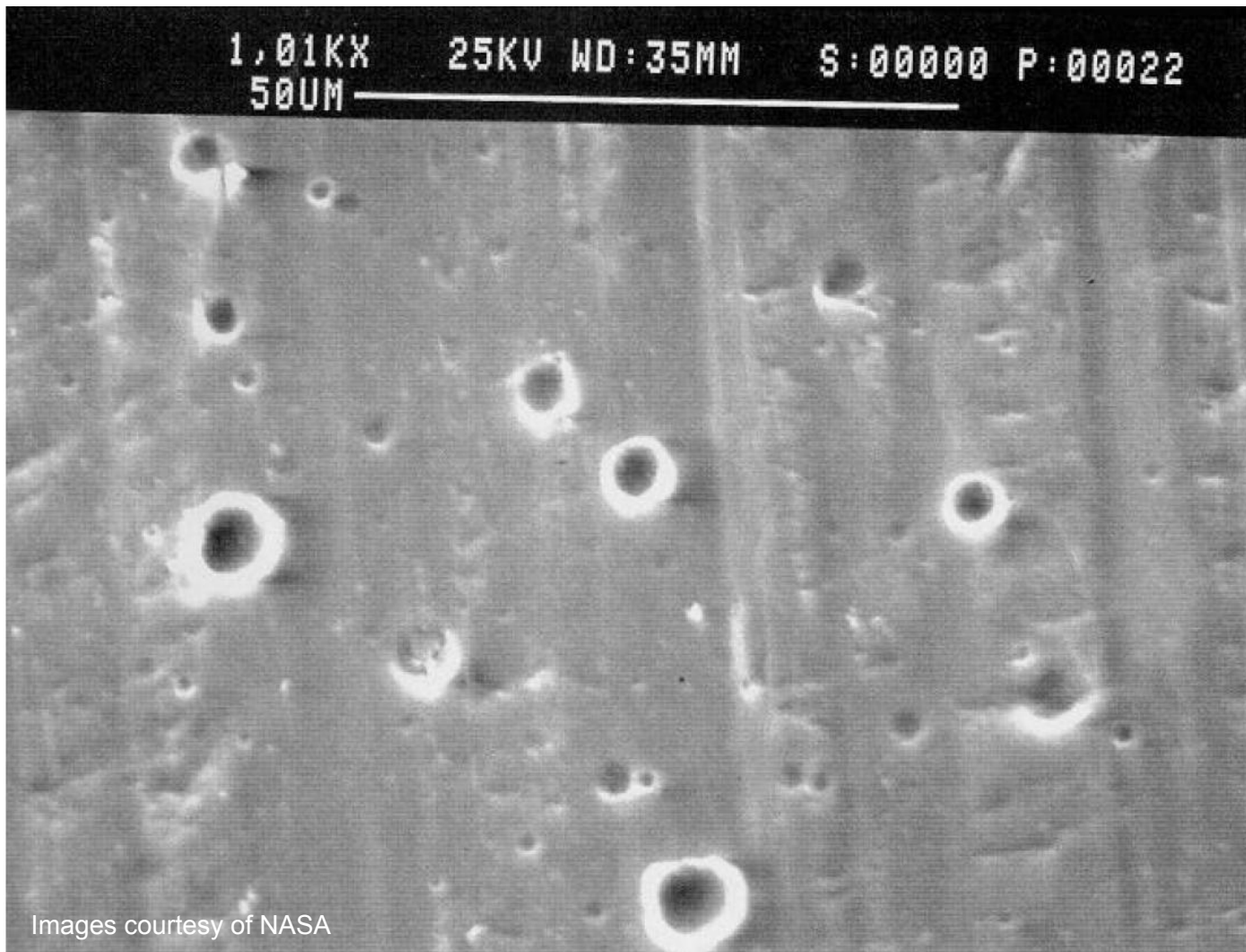




# Example SPIFEX Aluminum Foil Image: 1000x Magnification (50 $\mu\text{m}$ Scale)



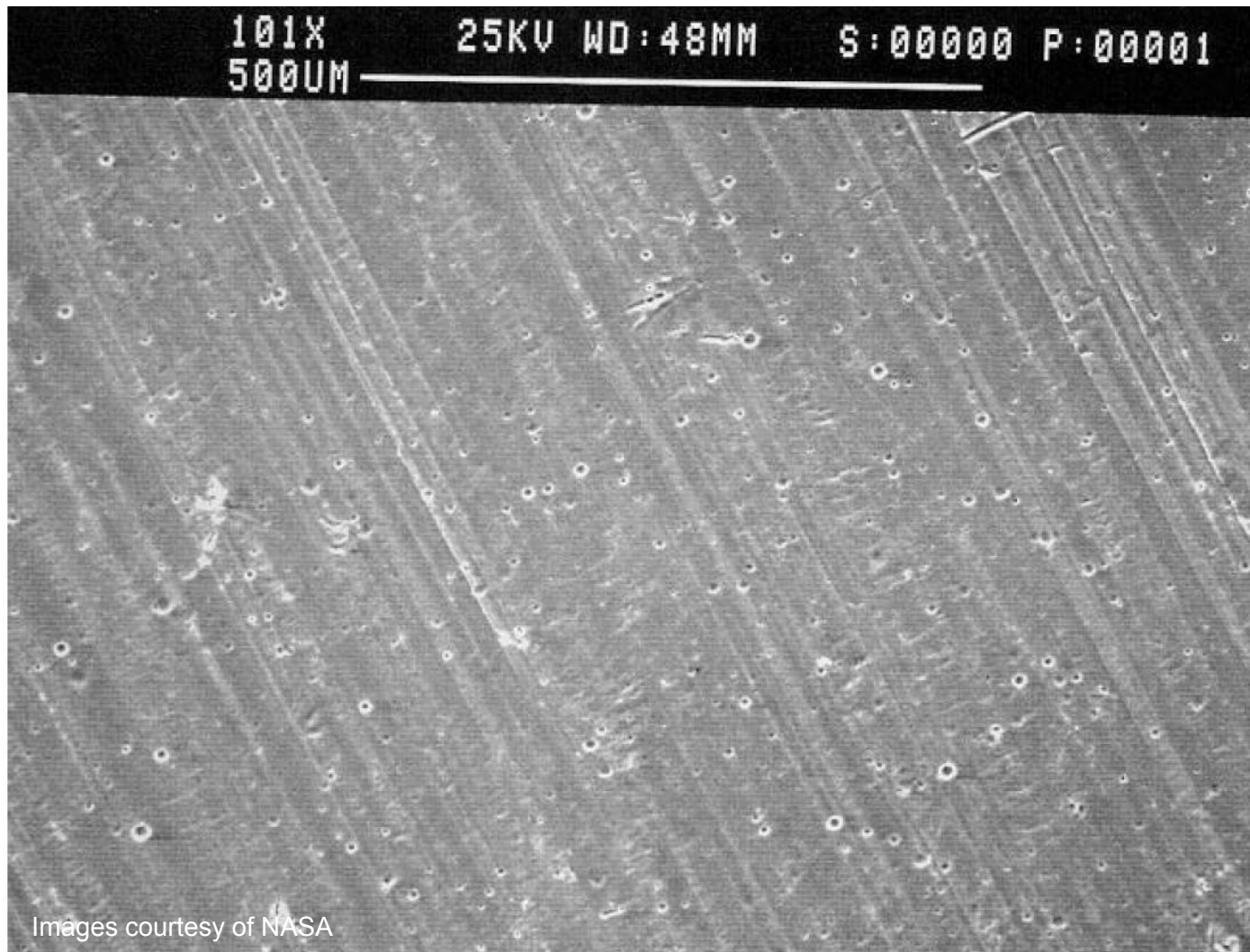
Engineering, Operations & Technology | Boeing Research & Technology



# Example SPIFEX Aluminum Foil Image: 100x Magnification (500 $\mu\text{m}$ Scale)



Engineering, Operations & Technology | Boeing Research & Technology





# SPIFEX Image Analysis Results

Engineering, Operations & Technology | Boeing Research & Technology



Sample	Approximate Pit Number Density Excluding Potential Pits (pits / mm <sup>2</sup> )	Approximate Pit Number Density Including Potential Pits (pits / mm <sup>2</sup> )
Kapton Tape	6710	9300
Aluminum Foil	2160	2160

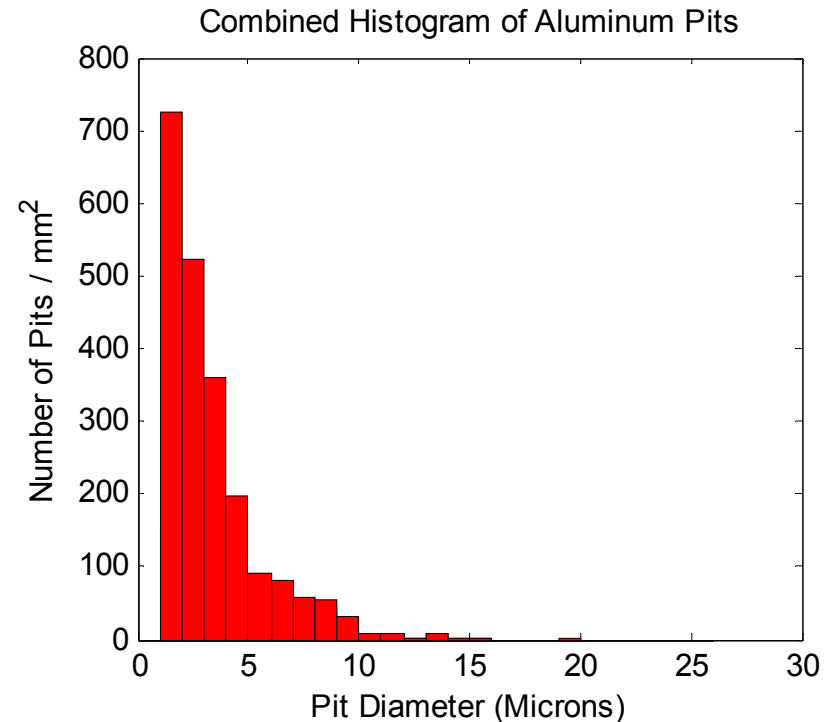
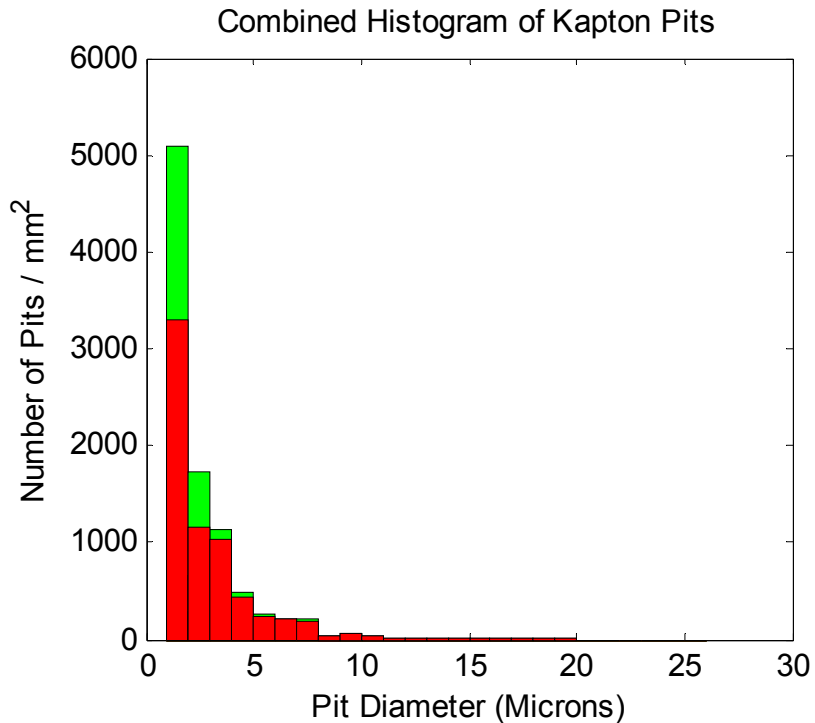
Note: Pit density rounded to the nearest multiple of ten pits / mm<sup>2</sup>

Sample	Approximate % Total Area Pitted Excluding Potential Pits	Approximate % Total Area Pitted Including Potential Pits
Kapton Tape	6.4%	7.5%
Aluminum Foil	2.8%	2.8%



# SPIFEX Image Analysis Results

Engineering, Operations & Technology | Boeing Research & Technology



Note: Histograms scaled to show similarities and differences in both distributions



# Summary of SPIFEX Image Analysis Results

Engineering, Operations & Technology | Boeing Research & Technology

- **Most common pit size is 1 – 2  $\mu\text{m}$**
- **Largest Kapton tape pit diameter is approximately 20  $\mu\text{m}$** 
  - Largest potential pit diameter is approximately 28  $\mu\text{m}$
- **Largest aluminum foil pit diameter is approximately 20  $\mu\text{m}$**
- **Both samples were exposed to the same thruster firings**
  - Can compare results to evaluate differences in material susceptibility to impact damage



# Comparison with Original Aluminum Foil Image Analysis Results (By KSC)

Engineering, Operations & Technology | Boeing Research & Technology

Comparison of number of pits identified per mm<sup>2</sup>

Pit Diameter	Original Count / mm <sup>2</sup>	Approximate Current Count / mm <sup>2</sup>
≤ 4 μm	449	1600
5 – 10 μm	231	320
11 – 20 μm	60	30

Reference: Soares, C., Barsamian, H., Rauer, S.: “*Thruster Plume Induced Contamination Measurements From the PIC and SPIFEX Flight Experiments*,” The Boeing Company, NASA JSC



# PIC Background

Engineering, Operations & Technology | Boeing Research & Technology

- **Conducted in 1996 (STS-74)**
- **Measured initial and permanent plume induced molecular contamination using Quartz Crystal Microbalances (QCM)**
- **Exposed QCM to:**
  - 20 PRCS firings
  - 100 Russian 130 N thruster firings
- **Impact features were observed on the camera lens of the Orbiter RMS**
  - Consistent with observations from the SPIFEX flight experiment

Soares, C., Barsamian, H., Rauer, S.: "*Thruster Plume Induced Contamination Measurements From the PIC and SPIFEX Flight Experiments*," The Boeing Company, NASA JSC





# PIC Statistics

Engineering, Operations & Technology | Boeing Research & Technology

- **61 pits / mm<sup>2</sup>**
- **Pitted area represents 1.8% of the camera lens surface area<sup>1</sup>**
- **PIC statistics given below**
  - 6 – 13  $\mu\text{m}$  bin is the most common PIC pit size
  - 2 – 3  $\mu\text{m}$  bin is the most common Hyzod pit size
  - 1 – 2  $\mu\text{m}$  bin is the most common SPIFEX pit size

Pit Diameter	Pit Density / mm <sup>2</sup>
2 - 5 $\mu\text{m}$	21
6 - 13 $\mu\text{m}$	30
14 - 24 $\mu\text{m}$	10

PIC Camera Lens Pit Density

1. Soares, C., Barsamian, H., Rauer, S.: "Thruster Plume Induced Contamination Measurements From the PIC and SPIFEX Flight Experiments," The Boeing Company, NASA JSC

